Scanning Microscopy

Volume 2 | Number 4 Article 8

11-7-1988

Monte Carlo Calculations of Secondary Electron Emission

Suichu Luo
University of Tennessee

David C. Joy
University of Tennessee

Scanning Microscopy, Vol. 2, No. 4, 1988 (Pages 1901-1915) 0891-7035/88$3.00+.00
Scanning Microscopy International, Chicago (AMF O'Hare), IL 60666 USA

MONTE CARLO CALCULATIONS OF SECONDARY ELECTRON EMISSION

Suichu Luo+ and David C. Joy*

EM Facility, University of Tennessee
Knoxville, TN 37996 and:

+Permanent Address: Dept. of Physics, Beijing Broadcasting Institute, Beijing China
* Metals and Ceramics Division, Oak Ridge National Laboratory, Oak Ridge, TN 37831

(Received for publication April 07, 1988, and in revised form November 07, 1988)

Abstract

Monte Carlo calculations of slow secondary electron (SE) generation have been performed. Construction of a model for SE production involves three distinct steps, determining the trajectory of the incident electron, computing the rate of secondary electron generation along the trajectory of both primary and backscattered electrons, and finally calculating the secondary electron emission by using a hybrid model of the exponential decay law and cascade process. The incident electron trajectory is computed using a plural scattering Monte Carlo model. For secondary electron generation our models take into account all possible creation processes of SE resulting from the interaction of primary and backscattered electrons with free as well as bound (core) electrons and from the volume plasmon decay. Calculated SE yields, energy distributions, angular and depth distributions for Au,Ag Cu and Al are in good agreement with the experimental data available in the literature.

Key Words: Monte Carlo simulation, secondary electrons, secondary electron distribution, backscattered electrons, core electrons, plasmons

***Address for correspondence:**
D.C. Joy, EM Facility,Walters Life Sciences Building,
University of Tennessee, Knoxville, TN 37996-0810,U.S.A.
Phone No. (615)-974-3638

Introduction

Advances in electron-optical and vacuum design have recently resulted in the availability of scanning electron microscopes with a potential spatial resolution of better than one nanometer. This level of performance has, in turn, stimulated renewed interest in the use of, and the limits to, secondary electron imaging in the SEM. This paper describes a Monte Carlo simulation which attempts to calculate from a detailed model of the electron beam interaction the properties of the secondary electron signal, such as its magnitude, and its angular and depth distribution, which are important in interpreting SE (secondary electron) images.

There have been several previous treatments of SE emission. Among them some are based on analytical or semianalytical models such as Wolff (1954), Amelio (1970), Cailler and Ganachaud (1972), Chung and Everhart (1974,1977), Bindi et al. (1980 a,b,c), Schou (1980,1988), Rosler and Brauer (1981a,b), Devooght et al. (1987) and some have been carried out with Monte Carlo simulation, for example Murata (1973), Koshikawa and Shimizu (1974), Shimizu et al. (1976), Murata et al. (1981), Ganachaud and Cailler (1979), Joy (1984,1985,1987 a,b), Luo et al. (1987), Ding and Shimizu (1988). Chung and Everhart (1974) calculated the energy distribution of SE using a simple exponential decay law to account for the escape process of the secondaries. Koshikawa and Shimizu (1974) investigated the use of a cascade process to describe the SE excitation mechanism. Joy (1984, 1985) incorporated the exponential decay law into a single-scattering Monte Carlo simulation and followed the trajectories of both primary and fast secondary electrons, although secondaries were only tracked to an energy of 200 eV. In most of these calculations the effect of backscattered electrons on secondary generation was only included indirectly. More recently (Joy 1987a) a Monte Carlo model using the exponential decay law, and assuming that secondary generation is proportional to electron stopping power, has correctly accounted for the effects of backscattering but the model itself is too generic to

Table of symbols

A Atomic weight (Eqs.1 and 2)
A1 Constant (Eq.10)
a Thickness of a monolayer of the sample (Eq.12)
a_0 Bohr radius (Eq.7)
B A number chosen by experiment (Eq.18)
D(E,$\hbar\omega$p,$\Gamma\upsilon$) Probability of plasmon decay via one-electron transitions (Eq.8)
E Electron energy
E0 Incident electron energy
E_0^G A variable in D(E,$\hbar\omega$p,$\Gamma\upsilon$) (Eqs.8 and 9)
EF Fermi energy
Ej Binding energy of the core electron
E(k) Energy of incident electron at the k-th step (Eq. 17)
E' Energy losses of the primary electron (Eqs.4 and 5)
E" Energy of new SE produced in cascade process
$\overline{E}_{SE}$ Average energy of true secondary electron (Table 4)
e Charge of an electron (Eqs.4 and 5)
$\vec{G}$ Reciprocal-lattice vector (Eqs.8 and 9)
J Mean ionization potential (Eqs.1,2 and 3)
K_0 $\hbar K_0$ is momentum of incident electron
m Mass of an electron (Eq.9)
$n_{\vec{G}}$ Number of equivalent reciprocal lattice vectors corresponding to $\vec{G}$ (Eq.8)
p Momentum of SE (Eq.22)
pc Critical normal component of momentum for SE to escape out of sample surface
p(E) Probability of crossing surface potential barrier for SE with energy E (Eq.16)
p(z) Probability of SE to penetrate a distance z retaining its energy (Eq.10)

Table of symbols

q0 Constant
q1 Constant
RND An equidistributed random number between 0 and 1 (Eqs.17 and 19)
S The product of path of incident electron and mass density of sample, i.e. S=sρ. (Eqs.1 and 2)
s The path of incident electron along trajectory
W_G The Gth Fourier coefficient of the lattice pseudopotential(Eqs.8 and 9)
Z Atomic number (Eqs.1,2 and 3)
z Depth of electron below surface (Eqs.10,11,13,14 and 15)
α Elastic scattering angle of incident electron (Eq.17)
β Efficiency factor for SE production by backscattered electrons
$\Gamma\upsilon$ Defined by Chung and Everhart (1977) (Eqs.6 and 8)
δ Total yield of SE
δcore Yield of SE excited from core electron
δd Yield of SE excited from d electron
δSE1 Yield of SE excited by incident primary electron
δvalence Yield of SE excited from valence electron
η Yield of backscattered electron
θc Critical angle for internal SE to escape out of sample surface
θ1 Defined by Chung and Everhart (1977) (Eqs.6 and 7)
θE The ratio of energy loss of incident electron to twice energy of incident electron , i.e., $\theta E=\Delta E/2E$. (Eq.7)
λ(E) Inelastic mean free path (Eqs.6,10,11,12,13,14and 15)
λeff(E0,θ1) Mean free path for creating long-wavelength plasmons(Eqs.6, 7)
ρ Mass density of sample
σ(E') Cross section for electron-electron inelastic collision (Eqs.4 and 5)
ϕ Workfunction (Eq.16)
$\hbar\omega$p Plasmon energy (Eqs.6,7,8 and 9)

permit detailed computation of some important specific aspects of SE emission.

In this paper the contribution of backscattered electrons has been taken into account, secondaries resulting from the interaction of both primary and backscattered electrons with free (valence) and bound (core) electrons and volume plasmons are considered, and the exponential decay law has been combined with the cascade process. The model provides data on secondary and backscatter yields as a function of beam energy, and on the energy, angular and depth distributions of SE, together with information on the relative importance of various contributions to these distributions. Data is presented for Al, Cu, Ag and Au for incident energies in the range 1 to 28 keV.

Model for SE emission

The electron range for a given beam energy E (28, 20, 15, 10 keV) is obtained from the Bethe (1930) equation

$$\frac{dE}{dS} = \frac{-7850}{E}\cdot\frac{Z}{A}\cdot\ln\left\{1.166\frac{E}{J}\right\}$$

$$(E_0>E>1.03J) \qquad (1)$$

and the empirical formula (Rao-Sahib & Wittry, 1974)

$$\frac{dE}{dS} = \frac{-6236}{E^{1/2}}\cdot\frac{Z}{A}\cdot J^{-1/2}$$

$$(1.03J>E>0.01keV) \qquad (2)$$

Where Z and A are the atomic number and the atomic weight, respectively, S= ρs, where s is the path along the trajectory(in m), ρ is mass density (in kg/m3) and J is the mean ionization potential (in keV). E is the energy of incident electrons (in keV) and the stopping power is then in keV.m²/kg. Following Myklebust et al. (1979) J can be written as:

$$J = 0.001[8.76Z+(58.8/Z^{0.19})] \qquad (3)$$

where J is in keV.The range determined from an integration of equations (1) and (2) is then divided into one hundred steps of equal length. The screened Rutherford cross section is used to determine the elastic scattering. 5000 trajectories (at normal incidence) are computed. For low incident energies ($1 < E < 5keV$) equation (2) is used when $E < 6.34J$ (Joy 1987a). The range is divided into 50 steps of equal length. Again 5000 trajectories are computed.

The models in this paper take into account all possible creation processes of SE resulting from the interaction of primary electrons and backscattered electrons with free as well as bound (core) electrons and from the volume plasmon decay (for Al only because there is no complete theory for Au, Ag and Cu). The differential cross section for production of SE from valence and d electrons for Au, Ag and Cu is given by Luo et al. (1987):

$$d\sigma(E') = \left(\frac{1}{4\pi\varepsilon_0}\right)^2 \frac{\pi e^4\, dE'}{E\,E'^2} \qquad (4)$$

Gryzinski's function (Gryzinski, 1965) is employed to describe the excitation of the core electron:

$$d\sigma(E') = \left(\frac{1}{4\pi\varepsilon_0}\right)^2 \frac{\pi e^4 E_j}{E'^3 E}\left(\frac{E}{E+E_j}\right)^{\frac{3}{2}}\left(1-\frac{E'}{E}\right)^{\frac{E_j}{(E_j+E)}}$$

$$\times\left\{\frac{E'}{E_j}\left(1-\frac{E_j}{E}\right)+\frac{4}{3}\ln\left[2.7+\left(\frac{E-E'}{E_j}\right)^{\frac{1}{2}}\right]\right\}dE' \qquad (5)$$

where E' is the energy losses of the primary electron and Ej is the binding energy of the core electron.

For aluminum , we have adopted the theoretical analysis made by Chung and Everhart (1977). The differential inverse mean free path or probability per distance creating SE's by volume-plasmon decay is:

$$\frac{d(1/\lambda)}{dE} = \lambda_{eff}^{-1}(E_0,\theta_1)\, D(E,h\omega_p,\Gamma_\upsilon) \qquad (6)$$

where

$$\lambda_{eff}(E_0,\theta_1) = \frac{2a_0E_0}{h\omega_p}\left[\ln\left(\frac{\theta_1^2+\theta_E^2}{\theta_E^2}\right)\right]^{-1} \qquad (7)$$

and $D(E,h\omega_\pi,\Gamma\upsilon)$ which describes plasmon decay via one -electron transitions is:

$$D(E,h\omega_p,\Gamma_\upsilon)=\left\{\sum_{\vec{G}} n_{\vec{G}}|w_{\vec{G}}|^2\right.$$

$$\left.\left[\tan^{-1}\left(\frac{E-E_0^G-h\omega_p}{\Gamma_\upsilon/2}\right)-\tan^{-1}\left(\frac{E-E_F-h\omega_p}{\Gamma_\upsilon/2}\right)\right]\right\}$$

$$\times\left\{\pi\sum_{\vec{G}} n_{\vec{G}}|W_{\vec{G}}|^2(E_F-E_0^G)\right\}^{-1} \qquad (8)$$

and

$$E_0^G = \frac{(h\omega_p-h^2G^2/2m)^2-4|W_{\vec{G}}|^2}{2h^2G^2/m} \qquad (9)$$

$h\omega_p$ is the plasmon energy, E_0 is the primary electron energy, a_0 is the Bohr radius. In Chung and Everhart (1977), E_0 was 1 or 2 keV, $\theta_E=q_0/K_0$, $(\theta_1^2+\theta_E^2)^{1/2}=q_1/K_0$, $q_1=2$ nm^{-1}, and $q_0=1.5$ nm^{-1} and we have used this data for E_0 up to 5 keV. (Note that Eqs. (6),(7),(8),(9) are Eqs. (22),(19),(23) and (24) of Chung and Everhart (1977) respectively)

For the calculation of $D(E,h\omega_p,\Gamma\upsilon)$ we have followed the procedures of Ashcroft and Sturm (1971), and Koyama and Smith (1970), considering only the eight equivalent reciprocal-lattice vectors G_{111} and G_{200} for Al with $n_{111}=8$ and $n_{200}=6$. Besides the SE produced by the incident primary electrons from volume plasmon decay, the new SE excited from volume plasmon decay by the internal SE in cascade process also has been calculated. The contribution of surface plasmon decay for SE is so small (see Chung and Everhart 1977) that it can be neglected.

An assumption in most SE theories is that secondary escape is governed by a function of the type

$$p(z) = A_1 \exp(-z/\lambda) \qquad (10)$$

This is a straight-line approximation, i.e., the emerging secondaries are unscattered on their way to the surface. It assumes that any scattering of an excited SE with the electron gas in the solid produces absorption; only those electrons that are not scattered between their points of excitation and the surface can escape (Chung and Everhart, 1974). In fact the scattering of excited SE does not produce absorption of all these SE. To improve this approximation, Chung and Everhart (1977) considered the contribution of singly scattered SE, but their theoretical values are still too low by roughly a factor of 3. In this paper the calculation of slow SE has been performed with a hybrid model of the exponential decay law and cascade process. The exponential decay is the statistical result of a cascade process. $p(z) = \exp(-z/\lambda)$ is the probability that SE penetrates a distance z along a straight line retaining its energy E. There is thus a total probability $\{1 - \exp(-z/\lambda)\}$ for a SE to take part in the cascade process. By considering the probability that a SE takes part in the cascade process the simple exponential decay expression can be improved.

The hybrid model of the exponential decay law and cascade process can be summarized as follows.

(1) The probability of arriving at the surface without any inelastic collision with the electron gas is

$$1/2 \exp(-z/\lambda\cos45^o) \qquad (11)$$

where 45^0 is an average escape angle and $\lambda(E)$ is the inelastic mean free path in metals which can be expressed as (Seah and Dench, 1979):

$$\lambda(E) = a\left\{ \frac{538}{(E-E_F)^2} + 0.41[a(E-E_F)]^{1/2} \right\} \qquad (12)$$

where E_F is the Fermi energy and a is the thickness of a monolayer of the target . E and E_F are in eV and with a in nanometers, $\lambda(E)$ is also in nanometers.

(2) The cascade process is described as follows:

The probability Pz' for a SE with energy E to travel from z to z' without any collisions is

$$1/2 \exp(-|z-z'|/\lambda(E)\cos45^o) \qquad (13)$$

The probability $P_{z+\Delta z'}$ for the SE to travel from z to $z' + \Delta z'$ without any collision is

$$1/2 \exp(-|z-(z'+\Delta z')|/\lambda(E)\cos45^o) \qquad (14)$$

so that between z' and $z' + \Delta z'$ the probability for the SE to interact with valence electron is

$$\Delta p_{z'} = p_{z'} - p_{z'+\Delta z'} = p_{z'}.\Delta z'/\lambda(E)\cos45^o \qquad (15)$$

$\Delta Pz'$ is the probability for the SE to travel from z' to $z' + \Delta z'$ to take part in the cascade process.

Following Luo et al. (1987) for each electron with energy E undergoing the cascade process, the probability of producing a new SE with energy E" is $\Delta E"/E$ (E" is in the energy interval [E", E"+dE"] and E" can vary from $E_F+\phi$ to E (if E<2keV) or 2 keV (if E>2 keV)) . For incident energies of 10, 15, 20 and 28 keV secondary electrons produced from valence and core electrons with energies lower than 2 keV are considered; for incident energies of 1,2,3 and 5 keV only SEs with energies up to 100 eV are calculated.

In order to overcome the surface barrier E must be greater than a critical value $E_F+\phi$. For a SE with energy E at the surface the probability of crossing the potential barrier is then

$$p(E) = 1 - \sqrt{\frac{E_F+\phi}{E}} \qquad (16)$$

A program incorporating all of these operations was written in Turbo PASCAL and run on an AT&T 6300 PC fitted with an 8087 maths coprocessor chip. Since the precision of the results from any Monte Carlo procedure has an error which is inversely proportional to the number of events simulated it is necessary to compute at least 2000 to 3000 trajectories to achieve a precision of a few percent. 5000 trajectories were used for all the data shown in this paper. Typical computation times were of the order of 25 minutes per data point.

Results and Discussion

(1) The calculations for the yield of BS are shown in Fig. 1.

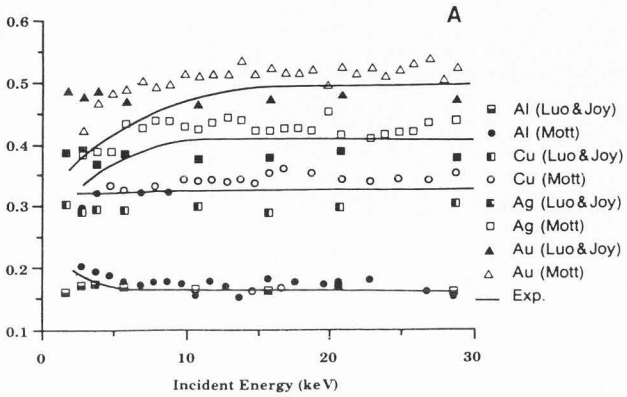

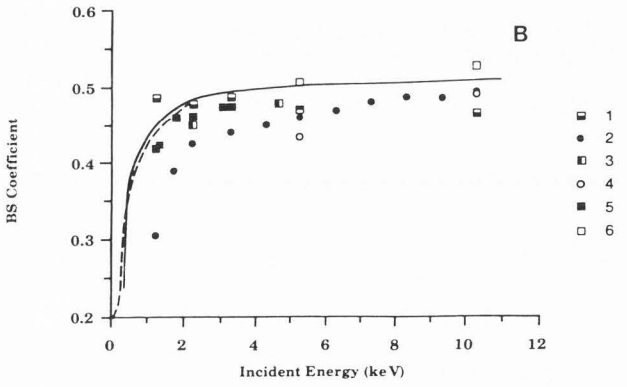

Fig. 1. (A) Comparison of our calculated yield η of BS using screened Rutherford cross section, with experimental data (Reimer and Tollkamp 1980 quoted from Reimer and Stelter 1986) and the values using Mott cross section (Reimer and Stelter 1986).

(B) Comparison of our calculated backscattered electron yield η for Au with experimental data and with values using the Mott cross-section. 1: our data, Experimental data: 2 :Reimer; 3 :Bronshtein and Fraiman; 4 : Cosslett and Thomas; 5 : Schou and Sorensen; 6 : Bishop; 7 : The data shown as ------ is from Thomas and Pattinson. The data —— is from a Monte Carlo calculation by Kotera et al. 1981. Data points 2, 3, 4, 5, 6 and 7 are quoted from Kotera et al. (1981).

η can be calculated using either the Rutherford or the Mott cross section . From Fig.1 it can be seen that the result of using a screened Rutherford cross section, and making the appropriate choice of the transition energy between the Bethe and Rao-Sahib-Wittry energy loss equations, is nearly as good as when using the Mott cross section from 1 to 28 keV. It is certainly true that at low energy and for high atomic number materials, the Mott cross section is expected to be more accurate (Krefting and Reimer 1973). However the quality of experimental data on η vs energy is such (Joy 1987b) that discrepancies between the Mott and Rutherford models are less than the uncertainty in measurements. We have therefore opted to use the model which is quickest and easiest and which, for the purposes of this paper, is certainly of adequate precision.

(2) The calculated yield δ of SE for Al, Cu, Ag and Au from 1 keV to 28 keV is shown in Table 1. The calculated results for the yield of SE are compared with experimental and the other theoretical predictions in Tables 2, 3 and 4, and are found to be in good agreement with these previous determinations. Fig. 2 shows the variation of the yield of SE and the yield of BS with beam energy for Al, where the Al-SE-yield is total yield of SE produced from all possible interactions; the Al-SE1-yield is the yield of SE excited from all possible interactions only by incident electron . At 1 and 2 keV the model used here gives a figure for the yield of SE for Al which is closer to experiment than that of Chung and Everhart (1977).

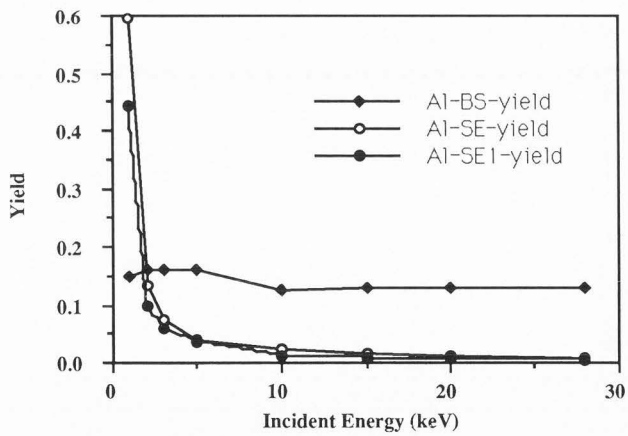

Fig. 2. The variation of the yield of SE and the yield of BS with beam energy for Al. Al-SE-yield is the total yield of SE; Al-SEl-yield is the yield of SE excited only by incident electron.

This is because the model also includes the excitation of new SE by the plasmon decay throughout the whole cascade process, instead of considering only single scattering, and this leads to an improvement of the calculated results for the SE yields from Al. Our computed data for the yield of SE for Au and Cu at 1,2 keV is also favorable in comparison with that of Bindi

Table 1. The yield of SE for Al, Cu, Ag and Au

Inc-energy in keV	1	2	3	5	10	15	20	28
Al	0.5963	0.1340	0.0736	0.0397	0.0236	0.0150	0.0112	0.0077
Cu	1.3047	0.5153	0.1652	0.0592	0.2459	0.1153	0.0838	0.0610
Ag	1.7526	0.9492	0.2767	0.0745	0.3340	0.1737	0.1292	0.0812
Au	1.9741	1.4617	0.6106	0.1588	0.4909	0.2649	0.1531	0.1122

Table 2. The yield of SE for Cu and Au

Inc-energy in keV		1	2
Cu	calc.	1.3047*	0.5153*
	calc.	0.18**	0.13** (1.8keV)
	exp.	0.86-1.07***	
Au	calc.	1.9741*	1.4617*
		0.28**	0.26** (1.8 keV)
	exp.	1.23-1.36***	1.15-1.18***(1.8 keV)

* our data
** by Bindi et al.(1980 a)
*** collected by Bindi et al. (1980 a)

Table 3. The yield of SE for Al

Inc-Energy in keV	1	2
cal.	0.5963*	0.1340*
	0.38**	0.18**
	0.37,0.52,0.57***	0.22,0.25,0.27***
	0.54#	0.345#
exp.	0.45****	0.23****
	0.60***	0.45***
	0.57**	0.39**
	0.50Δ	0.28##

*	our calculated data	**	Bronshtein and Fraiman (1969)
**	Bindi (1978)	Δ	Roptin (1975)
***	Bindi et al .(1980 c)	#	Schou (1988)
****	Bronshtein and Fraiman (1961)		

Table 4. Calculated and experimental results of SE at 28 keV

	Cu	Ag	Au	Al
δ calc.	0.0610	0.0812	0.1122	0.0077
exp.	0.095*	0.09*	0.17*	
	0.095**	0.13* (30keV)	0.13*	
β calc.	3.25	2.81	2.81	3.98
E_{SE}(ev) calc.	20.5	18.5	19.7	19.7

* collected by Reimer (1984)
** Reimer et al. (1968)

Table 5. The β of Al, Cu, Ag and Au

Inc.-energy in keV	1	2	3	5	10	15	20	28
Al calc.	2.31	2.43	1.76	1.05	6.03	4.93	4.62	3.98
	5*				3.56Δ			
Al exp.	4.6-7.2*	3.5***		2.0##(9.3keV)		2.1##(25.2keV)		
	7.9**	4***		2.5##(11keV)		2.4##(32.4keV)		
		6***			1.8##(13.4keV)			
					2.8##(17.3keV)			
Cu calc.	3.55	2.59	2.21	1.34	7.38	4.07	3.45	3.25
					3.41Δ			
Ag calc.	2.76	2.14	1.89	1.20	6.84	4.1	3.85	2.81
		25Δ	15Δ	5.55Δ	3.26Δ		3.54Δ	4.5Δ(30keV)
Au calc.	1.53	1.34	1.26	1.28	7.22	4.66	2.96	2.81
					3.07Δ			
Au exp.				1.9##(9.3keV)			2.9#(25.2keV)	
				1.7##(11keV)			2.3#(32.4keV)	
					1.6##(13.4keV)			
					2.1##(17.3keV)			

* Bindi et al. (1980b)
** Bronshtein and Fraiman (1961)
*** Rosler and Brauer (1981b)
\# Drescher et al.(1970)
Δ Joy (1987a)
Reimer and Drescher (1977)

et al. (1980a). Above 3 keV, however, the model predicts an SE yield for Al that is much lower than the experimental data. This is because we have not adequately considered those SE with energy above 100 eV, which can play an important role in creating a new internal SE by the plasmon decay. The formula used for predicting the probability of SE formation during the cascade, i.e., $\Delta E''/E$, is less accurate when applied to SE with energies as large as 2 keV, than to the lower energy cases (Luo et al. 1987).

(3) Obtaining the energy distribution curve (EDC) of the slow SE is important to any study of the properties of SE. In our models the total energy distribution, the energy distribution of SE excited by the incident electrons , by backscattered electrons, from valence, d(for Au, Ag and Cu) and core electrons, by incident electrons from plasmon decay and by plasmon decay only (for Al), can all be calculated simultaneously. Fig. 3 shows the energy distribution owing to these different excitation mechanisms, as well as the total distribution function. Curve 1 is the external EDC from the excitation of SE's in sample generated from the decay of volume plasmons, generated by the incident fast electrons, then multiplied by electron-electron interaction in cascade process; curve 2 is the total external EDC of SE, including all contributions by both incident and backscattered electrons, and by volume plasmon decay as well as electron-electron scattering; curve 3 is the external EDC from the excitation of SE's in sample via electron-electron scattering between the incident primary as well as backscattered electrons and crystal electrons, and multiplied through electron-electron interaction in cascade process; curve 4 is the EDC of external SE produced from the decay of volume plasmon by the incident primary and backscattered electrons, then multiplied from volume plasmon decay and electron-electron interaction in the cascade process.

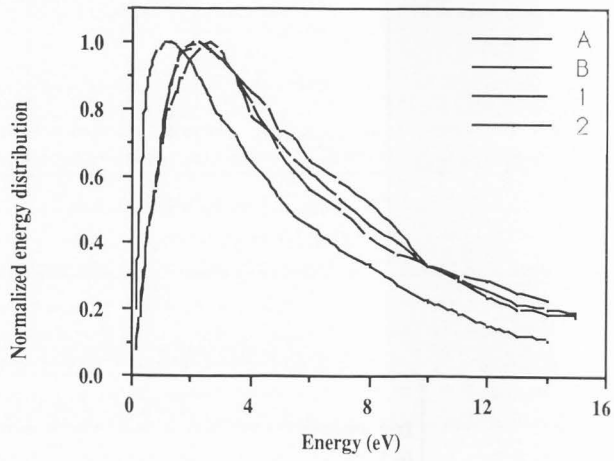

Fig. 4. Normalized secondary electron energy distribution curves from gold at 1 keV. **Curve 1**: present model; **Curve 2**: Bindi et al. model (1980a) Experimental curves: **A**: Bindi et al. (1980a) **B**: Pillon and Roptin's (quoted form Bindi et al. 1980a)

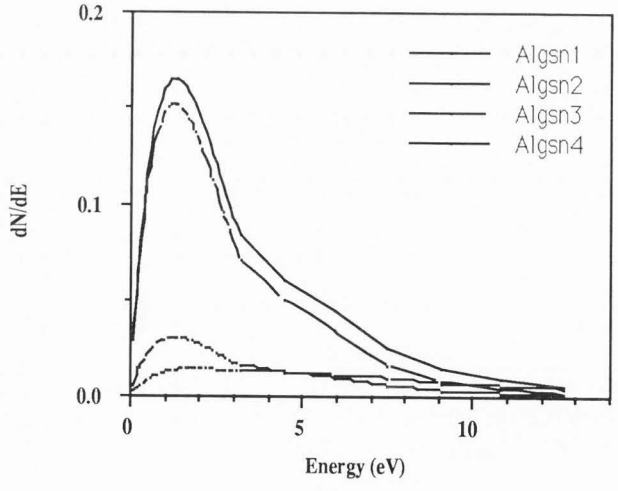

Fig. 3. The energy distribution of SE for Al at 1 keV Algsn1: the ED of SE excited from volume plasmon decay by incident electron; Algsn2: the total ED of SE; Algsn3: the ED of SE from electron-electron scattering only; Algsn4: the ED of SE from volume plasmon decay.

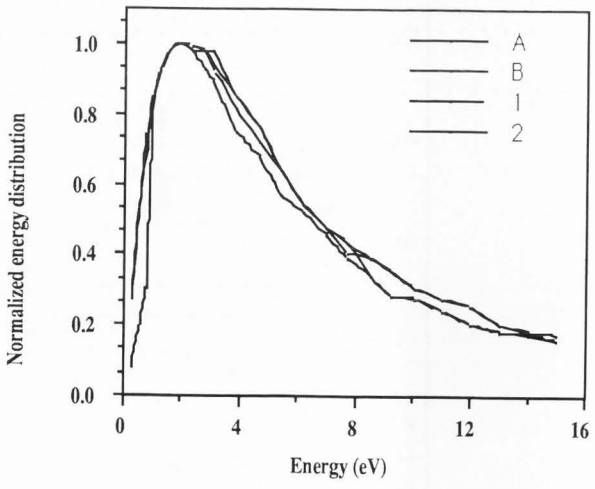

Fig. 5. Normalized secondary electron energy distribution curves from copper at 1 keV. **Curves 1**: present model; **2:** Bindi et al. (1980a); Experimental curves: **A**: Bindi et al. (1980a), **B**: Pillon and Roptin (quoted by Bindi et al. 1980a)

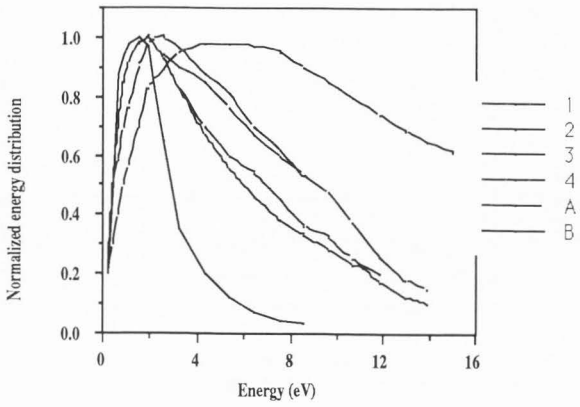

Fig. 6. Comparison of theoretical and experimental normalized energy distribution of SE for Al at 1 keV. Theoretical curves: **1.** present calculations; **2.** Bindi et al. (1980c); **3.** Chung and Everhart (1977); **4.** Amelio's model with corrections (quoted from Bindi et al. 1980c). Experimental curves: **A**: Bindi et al. (1980c); **B**: Roptin (1975).

Our EDC shows that the majority of the secondaries originates from plasmon decay. This is in agreement with the results of Chung and Everhart (1977 Fig.4) , Rosler and Brauer(1981b, p.586, Table 4) and Bindi et al. (1980c Fig.2). Figs.4 and 5 compare our ED curves with other models and the experimental data for Cu and Au demonstrating good agreement with the experimental results. Fig.6 shows our ED curve for Al with the other model data and the experimental data.

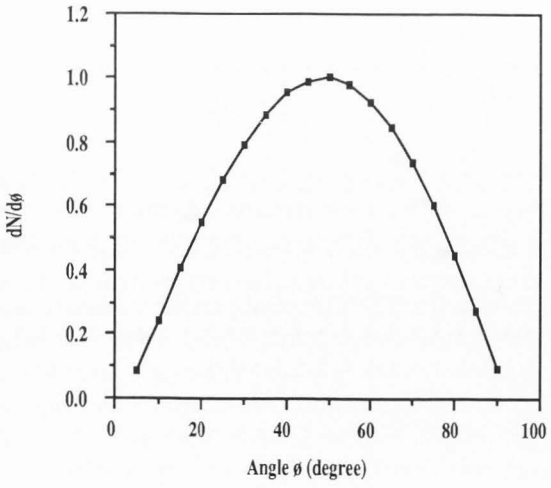

Fig. 7. The angular distribution of SE for Al at 2 keV.

(4) In fig. 7 is shown the angular distribution of SE for Al at 2 keV. We obtain a cosine distribution for all contributions from different excitation mechanisms and different shell electrons for Al, Cu, Ag and Au at all energy we calculated. This distribution mainly results from the elastic collisions of the low energy SE. It is a direct consequence of the isotropic distribution of internal SE.

(5) The depth distributions of SE for Al at 2 keV are depicted in Fig. 8. Curve 1 is the depth distribution for SE excited by the incident electrons. Curve 2 is by the backscattered electrons (both curves 1 and 2 include the contribution of volume plasmon decay). Few electrons excited in the region deeper than 50 nm can eject as SE's. This agrees with the results of Koshikawa and Shimizu (1974).

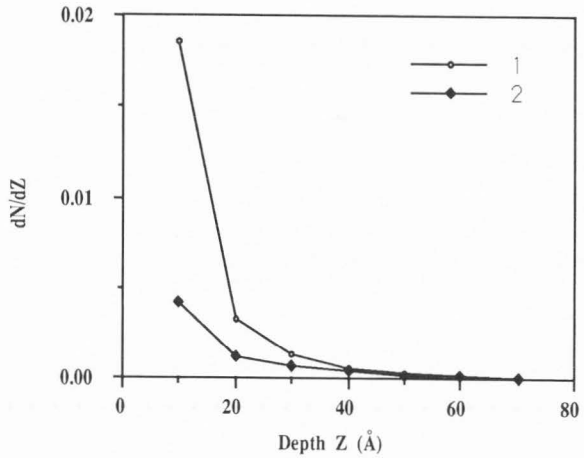

Fig. 8. The depth of distribution of SE for Al at 2 keV

(6) Figs.9, 10, 11 and 12 show the contribution to SE from valence, d and core electrons for Al, Cu, Ag and Au at different incident energies (the contribution of plasmon decay is not included). From Figs. 10 ,11 and 12 it can be seen for Cu, Ag and Au the d-electron is important for SE. About 40 - 80% of SE of Cu, Ag and Au are produced by the excited d-electrons. It is therefore not surprising that values of d calculated for Au without consideration of the d-electron contribution, are too low (Richard,1974 and Richard et al., 1975).

Cailler (1969, Cailler and Ganachaud 1972) was the first to consider the "d" electron contribution to SE production for the noble metals. Our calculations also support the comment of Bindi et al. (1987) that "...in the excitation process of SE, one has to consider the 'd' electron contribution of the noble metals." The SE excited from core electrons should also not be neglected. Figs. 9, 10, 11 and 12 show that not only for Cu, Ag and Au, but also for the low atomic number element Al

(except the contribution of plasmon decay), the fraction of SE excited from core electrons is rather high. For Al it is about 70% at keV and above, for Au about 60% at keV and above. Even at low incident energy they are still 40-50% for Au and 30-40% for Al.

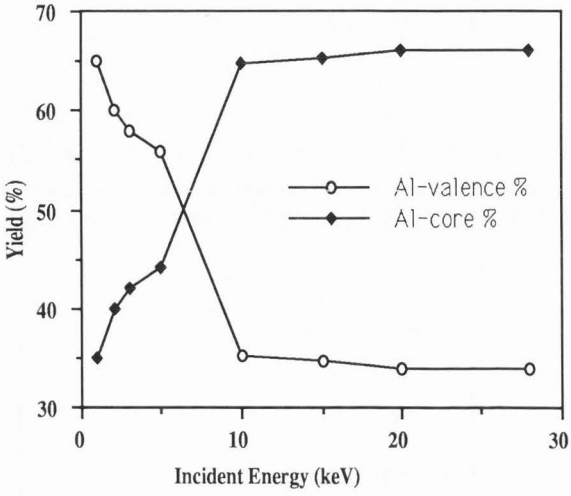

Fig. 9. The percent of SE from valence and core electrons for Al (the contribution of plasmon decay is not included) Al-valence: the percent of SE from valence electrons: Al-core: the percent of SE from core electrons.

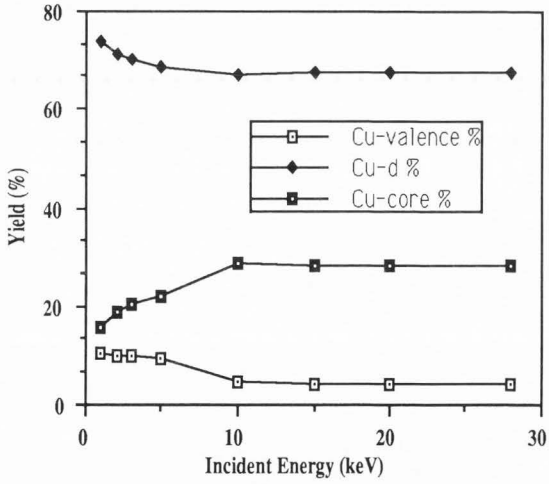

Fig. 10. The percent of SE from valence, d and core electrons for Cu. Cu-valence: the percent of SE from valence electrons; Cu-d the percent of SE from d-electrons; Cu-core: the percent of SE from core electrons.

(7) β is the ratio of the secondary yield per backscattered electron compared to the secondary yield per incident electron. Its value determines the fractional content of high resolution SE1 electron in the total secondary signal.

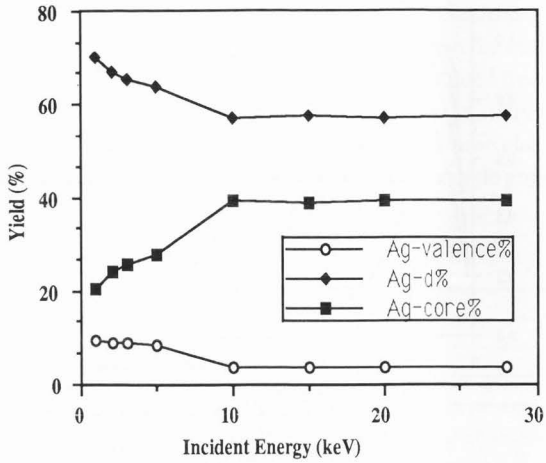

Fig. 11. The percent of SE from valence, d and core electrons for Ag. Ag-valence: the percent of SE from valence electrons; Ag-d: the percent of SE from d-electrons; Ag-core: the percent of SE from core electrons.

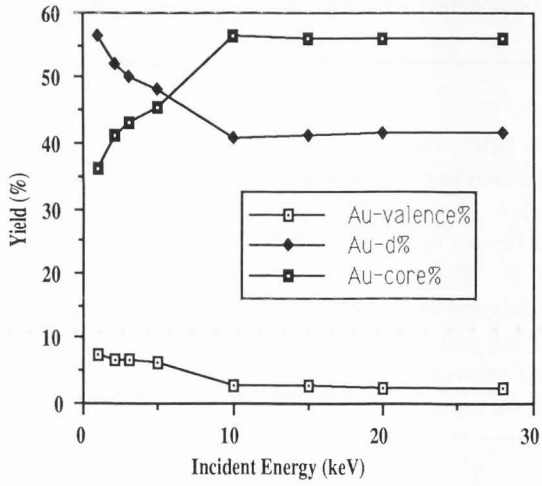

Fig. 12. The percent of SE from valence, d and core electrons for Ag. Ag-valence: the percent of SE from valence electrons; Ag-d: the percent of SE from d-electrons; Ag-core: the percent of SE from core electrons.

Table 5 lists values for β, computed at 1 to 28 keV for Al, Cu, Ag, Au and some experimental data showing good agreement. There is however a discontinuity in our data at 10 keV for the calculated values of β for all metals listed. This is because the energy of internal SE calculated is taken over a different range: for E_o from 1 to 5 keV the energy range is only taken up to 100 eV; but for E_o from 10 to 28 keV it is extended up to 2 keV. To reduce the magnitude of this discontinuity we need more accurate models for the contribution of internal SE with high energy in the cascade process, and work is proceeding on this aspect of the problem.

At present, our model is applied for metals only. But it is able to successfully calculate data such as: η , δ , δSE1, $\delta_{valence}/\delta$, δ_d/δ, and δ_{core}/δ ; the angular , depth, and energy distribution (for Al, Cu, Ag and Au) and the contribution to δ of plasmon decay (for the case of Al). In addition to the work now in progress on the contribution of the high energy SE, our model is expected to be improved for incident beam energies below 1 keV, and it is planned to extend its application to other materials, for example, metal oxides.

Conclusions

There have been two main theoretical treatments of secondary electron production in metals; those using Monte Carlo methods and those applying the Boltzmann transport equation. By using Boltzmann transport equation the computation of the backscatter contribution to the secondary production is more indirect than is the case for the Monte Carlo method. The Monte Carlo method thus has advantages when the contribution of backscattered electrons is important.

There have also been two distinct theoretical treatments of secondary electron production by Monte Carlo methods, involving the use of an exponential decay law or the cascade process. In the past these two methods have been considered to be different and have been used separately, and each has its own shortcoming. The exponential decay law assumes that any scattering of an excited SE with the electron gas produces absorption. Although they used the process model Koshikawa and Shimizu (1974) did not consider the contribution of SE excited by BS electrons or by internal SE with high energy (>100eV).

It is believed that this present paper represents one of the most complete approaches to the study of secondary electron emission based on the Monte Carlo method. A more detailed analysis of each elementary process can now be made in order to achieve better agreement between theory and experiment in each of the three stages of the analysis:

(1) the production of internal SE by collisions between fast primaries or BS electrons and valence,d,or core electrons, and from volume plasmon decay.

(2) the cascade process. The exponential decay law is adopted in the cascade process, not only to describe the diffusion of the SE through the solid to reach the surface, but also to calculate the probability of producing new SE.

(3) the transmission of the SE through the surface potential barrier.

It must be pointed out that, in this paper, the calculation of the high energy SE contribution is performed rather approximately, however no one except Joy (1984) has previously considered the contribution of high energy SE to the yield of SE in a Monte Carlo simulation. In previous papers (e.g., Chung and Everhart 1974,1977; Koshikawa and Shimizu 1974; Bindi et al. 1980a,b,c; Rosler and Brauer 1981a,b) only internal secondary electrons with energies below 100 eV are considered. Work is also in progress to adopt the procedures described here to the computation of SE yields in the low energy range 0.1 to 1 keV, and to generalize the applicability of the method to include semiconductors, insulators and oxides.

Finally it must be noted that the present body of experimental data for the energy variation of secondary and backscattered yields, the energy and angular distribution of secondaries, and other important variables is very limited. Systematic and detailed work is required to make such data available so that models of all types can be improved and their results properly evaluated.

Acnowledgement

This research was partially sponsored by the Division of Materials Sciences, US Department of Energy under contract DE-AC05-840R21400 with Martin Marietta Energy Systems Inc.

References

Amelio GF (1970) Theory for the energy distribution of secondary electrons. J. of Vac. Sci. and Technology **7**, 593-604.

Ashcroft NW, Sturm K (1971) Interband Absorption and the Optical Properties of Polyvalent metals. Phys. Rev. **B3**, 1898-1910.

Bethe H (1930) Theory of passage of swift corpuscular rays through matter. Ann. Phys. **5**, 235.

Bindi R (1978) Contribution a l'etude de l'emission electronique secondaire de cibles metalliques polycristallines. These d' Etat-Universite de Nice, France.

Bindi R, Lanteri H , Rostaing P (1980 a) Application of the Boltzmann equation to secondary electron emission from copper and gold. J. Phys. D : Appl. Phys., **13**, 461-470.

Bindi R, Lanteri H, Rostaing P, Keller P (1980 b) Theoretical efficiency of back-scattered electrons in secondary electron emission from aluminium. J. Phys. D: Appl. Phys., **13** , 2351-2361.

Bindi R, Lanteri H, Rostaing P (1980 c) A new approach and resolution method of the Boltzmann equation applied to secondary electron emission by reflection from polycrystalline aluminium. J. Phys. D: Appl. Phys., **13** , 267-280.

Bindi R, Lanteri H , Rostaing P (1987) Secondary electron emission induced by electron bombardment of polycrystalline metallic targets. Scanning Microscopy, **1**, 1475-1490.

Bronshtein IM , Fraiman BS (1961) Inelastic Scattering of electrons and secondary electron emission from certain metals and semiconductors. Sov. Phys. Solid State,**3**, 1188-1196.

Bronshtein IM , Fraiman BS (1969) Sekundarelektronenemition, Izd (Nauka, Moscow).

Cailler M (1969) Contribution a L'Etude theorique de L'emission electronique secondaire induite par bombardement electronique. -These d'Etat- Universite de Nantes-France.

Cailler M , Ganachaud JP (1972) Quelques aspects theoriques de L'emission electronique secondaire du cuivre produit par bombardement d'electrons de faible energie. J. Physique, **33** ,903-913.

Chen Yongqi, Mao Yunjin (1983) Monte Carlo Method and its application to electron probe microanalysis. J.Chinese EMS. **2** , 16-22 (in Chinese).

Chung MS , Everhart TE (1974) Simple calculation of energy distribution of low-energy secondary electrons emitted from metals under electron bombardment. J. Appl. Phys. **45**, 707-709.

Chung MS , Everhart TE (1977) Role of plasmon decay in secondary electron emission in the nearly-free-electron metals. Application to aluminum. Phys. Rev. B, **15**, 4699-4715.

Devooght J, Dubus A, Dehaes JC (1987) Improved age-diffusion model for low-energy electron transport in solids. Phys. Rev. B. **36** , 5093-5119.

Ding ZJ, Shimizu R (1988) Monte Carlo study of backscattering and secondary electron generation. Surf. Science, **197**, 539-554.

Drescher H, Reimer L, Seidel H (1970) Ruckstreukoeffizient und Sekundarelektronen Ausbeute Von 10-100 keV-Elektronen und Beziehungen zur Raster-Elektronenmikroskopie. Z. Angew Phys., **29,** 331-336.

Ganachaud JP , Cailler M (1979) A Monte Carlo calculation of the secondary electron emission of normal metals. Surf. Science. **83**,498-518.

Gryzinski M(1965) Classical theory of atomic collisions. I. Theory of inelastic collisions. Phys. Rev. A.,**138**, 336.

Joy DC (1984) Monte Carlo studies of high resolution imaging. In: Microbeam Analysis 1984 (Ed.) A. Romig , J. Goldstein, pp. 81-86. San Francisco, CA.

Joy DC (1985) Resolution in low voltage scanning electron microscopy. J. Microsc. **140**, 283-292.

Joy DC(1987a) A Model for Calculating Secondary and Backscatter Electron Yields. J. of Microscopy, **147**, p 51-64.

Joy DC (1987b) Low Voltage Scanning Electron Microscopy. In: Electron Microscopy and Microanalysis 1987. (Ed.) LM. Brown, Inst. Phys. Conf. Ser. **90**, p. 175-180.

Koshikawa T , Shimizu R (1974) A Monte Carlo calculation of low energy secondary electron emission from metals. J. Phys. D: Appl. Phys. **7**, 1303-1315.

Kotera M, Murata K, Nagami K (1981) Monte Carlo simulation of 1-10-keV electron scattering in a gold target. J.Appl. Phys.,**52** , 997-1003.

Koyama RY, Smith NV (1970) Photoemission Properties of Simple Metals. Phys. Rev. **B2**, 3049-3059.

Krefting ER, Reimer L (1973) Quantitative analysis with microprobe and secondary ion mass spectroscopy(Ed.) E. Preuss (Zentralbibliothk der K.F.A. Julich GmbH) p.114

Luo, S, Zhang, Y , Wu, Z (1987) A Monte Carlo calculation of secondary electrons emitted from Au, Ag and Cu. J. Microsc., **148**, 289-295.

Murata K (1973) Monte Carlo calculations on electron scattering and secondary electron production in the scanning electron microscope. Scanning Electron Microsc. 1973; 267-276.

Murata K, Kyser DF, Ting CH (1981) Monte Carlo simulation of fast secondary electron production in electron beam resists. J. Appl. Phys. **52**, 4396-4405.

Myklebust RL, Newbury DE , Yakowitz H (1979) The NBS Monte Carlo electron trajectory program. In: Use of Monte Carlo Calculations in EPMA and SEM. (ed.) KFJ. Heinrich, p. 105. NBS Special Publication 460,National Bureau of Standards, Washington, D.C.

Powell CJ (1976) Cross sections for ionization of inner-shell electrons by electrons. Rev. Mod. Phys. **48**, 33-47.

Rao-Sahib TS,Wittry DB (1974) X-ray continuum from thick elemental target. J. Appl. Phys., **45**, 5060.

Reimer L, Seidel H, Gilde H (1968) Einfluss der Elektronendiffusion ouf die Bildentsehung im Raster-Elektronenmikroskop. Beitr. Elektr.mikrosk. Direktabb. Oberfl. (Munster),**1,** 53.

Reimer L and Drescher H (1977) Secondary electron emission of 10-100 keV electrons from transparent films of Al and Au. J.Phys. D: Appl. Phys.,**10** , 805-815.

Reimer L (1984) Scanning Electron Microscopy, Quantitative E.M. Proceedings of Scottish Summer Schools Conference, ed A N Chapman, 22.

Reimer L, Stelter D (1986) Fortran 77 Monte Carlo program for minicomputers using Mott cross-sections. Scanning. **8** , 265-277.

Richard C (1974) Contribution a l'etude de l'emission electronique secondaire par bombardement electronique, sur des cibles d' Al et Au. These de Specialite-Universite de Marseille, France.

Richard C, Bindi R, Lanteri H, Keller P(1975) Rendement d'emission electronique secondaire deduit d'un modele analytique: comparaison avec Les valeurs experi-

mentales pour Au et Al. Thin Solid Films.**26**, 119-127.

Roptin D (1975) Etude experimentale de l'emission electronique secondaire de l'Aluminum et de l'Argent. These de Docteur-Ingenieur, Universite de Nantes, France.

Rosler M, Brauer W (1981a) Theory of Secondary Electron Emission I. General theory for nearly free electron metals. Phys. Stat. Solid. (b) **104** , 161-175.

Rosler M, Brauer W (1981b) Theory of Secondary Electron Emission II. Application to Aluminum. Phys. Stat. Sol. (b) **104**, 575-587.

Samoto N, Shimizu R (1983) Theoretical study of the ultimate resolution in electron beam lithography by Monte Carlo simulation, including secondary electron generation:Energy dissipation profile in polymethylmethacrylate. J.Appl.Phys. **54**,3855-3859.

Schou J (1980) Transport theory for kinetic emission of secondary electrons from solids. Phys.Rev.B.**22**, 2141-2147.

Schou J (1988) Secondary electron emission from solids by electron and proton bombardment. Scanning Microscopy,**2**, 607-632.

Seah MP, Dench WA (1979) Quantitative Electron Spectroscopy of Surfaces: A Standard Data Base for Electron Inelastic Mean Free Paths in Solids. Surf. Interface Analysis,**1** , 2-11.

Shimizu R, Murata K (1971) Monte Carlo calculations of the electron-sample interactions in the Scanning Electron Microscope. J. Appl. Phys.,**42** , 387-394.

Shimizu R, Kataoka Y, Ikuta T, Koshikawa T, Hashimoto H (1976) A Monte Carlo approach to the direct simulation of electron penetration in solids. J.Phys.D: Appl.Phys. **9**,101-114.

Wolff PA (1954) Theory of secondary electron cascade in metals. Phys.Rev.**95**,56-66.

Discussion with Reviewers

J.Schou: Is it possible to incorporate recent improvements of the electron stopping power(conf.the work of R.Nieminen) into your model instead of Eq.(2)?

Authors: We would like to consider your question but the reference you suggested was unavailable to us.

J.Schou: How is the angle θ defined? Usually one expects a cosine-distribution to have a maximum at $\theta=0^o$ (for a direction perpendicular to the surface).

Authors: The angle θ is defined as the angle between the normal direction to sample surface and the direction of a SE moving out of the sample. Our calculation of the cosine-angular distribution is the same as those calculated by Koshikawa and Shimizu (1974), Bindi et al.(1980c) and Rosler and Brauer (1981b) where $f(\theta)$ is the angular distribution, one can expect $f(\theta)$ to have a maximum at $\theta=0^o$ (for a direction perpendicular to the surface). Then $f(\theta)\sin\theta d\theta d\varphi$ represents the number of electrons coming into the solid angle $\sin\theta d\theta d\varphi$. In our Fig.7 we plot the data $dN/d\theta = 2\pi\phi(\theta)\sin\theta$ directly.

R.Bindi: Could the authors describe how they distinguish the contribution of incident primary and backscattered electrons in S.E.E. ?

Authors: In our model the incident electron trajectory is computed using a plural scattering Monte Carlo model. The electron range for a given beam energy E_0 is obtained from the Bethe (1930) equation and Rao-Sahib and Wittry(1974) empirical formula. The range is then divided into 100 (above 10 keV) or 50 (below 5 keV) steps of equal length. For accuracy we record both path along trajectory and energy of the incident electron from surface down to 14 nm which is much deeper than a typical low-energy SE escape depth (~ 5 nm in most metals). We assume the path along its trajectory throughout 14 nm as the primary electron path when an incident electron enters sample, the rest of path along trajectory recorded between 0 and 14 nm as the backscattered path (including those path of electrons which are backscattered out of sample or stay in the sample and have its zig-zag path in 14nm). According to the path and energy of incident primary electrons or backscattered electrons the rate of secondary electron generation along the trajectory of both primary and backscattered electrons can be calculated directly.

R.Bindi: How do you take into account the elastic collisions of the primary electrons and low energy S.E. in your Monte Carlo calculation ?

Authors: In our plural scattering Monte Carlo method of incident electron we assume that inelastic scattering leads to the energy losses rather than direction change for an incident electron. The direction change of incident electron is controlled by elastic scattering only. A screened Rutherford cross-section is used to determine the elastic scattering. The electron, at the start of the k-th step is deflected through an angle a given(Myklebust et al. 1979) as

$$\tan(\alpha/2) = \frac{B}{E(k)}\cdot\left[\frac{1}{\sqrt{RND}} - 1\right] \qquad (17)$$

where RND is an equidistributed random number between 0 and 1, and B is chosen so that the computed backscattered coefficients match those obtained experimentally. Here

$$B = 0.237\, Z^{0.6} \qquad (18)$$

as given by Myklebust et al. (1979). With this choice a good fit is obtained to tabulated backscattering data for all elements between carbon and gold. Scattering can also occur in any azimuthal direction φ, where

$$\varphi = 2\pi \text{ RND} \qquad (19)$$

and RND is a second, independent, random number. Given the two scattering angles, the step length and starting coordinates, the end coordinates of the k-th step can be found, and the procedure repeated until the electron reaches the end of its range, or is backscattered out of the sample.

As to the elastic collisions of low energy SE, We agree with Samoto and Shimizu(1983) , they said that " We did not simulate the elastic scattering process for the secondary electrons because the mean free path of the slow secondaries becomes as small as the order of atomic distance, leading to an isotropic diffusion." We do not simulate the elastic scattering process for SE in cascade process directly too. We think the main results of elastic collision is isotropic of SE movement and a more zig-zag path in the sample for SE. These two have been considered in our calculation: in cascade process the probability for SE to travel a distance z without any inelastic collision is $1/2 \exp(-z/\lambda \cos 45^0)$ instead of $1/2 \exp(-z/\lambda)$, where 45^0 is an average escape angle, λ is the inelastic mean free path. The average angle 45^0 results from the isotropic elastic diffusion at the same time it represents the zig-zag path (because its path is $z/\cos 45^0$ instead of z).

R.Bindi: I think the cascade process and the contribution of fast secondary electrons generated from the interaction of primary electrons with core electrons are over estimated, specially for low primary energy.

For instance, in the range 0.5-3 keV the ionization mean free paths, for Al and Cu, are much greater than inelastic mean free paths for both individual and collective excitation and also much greater than elastic mean free path. So the probability of an ionizing collision is clearly weak. For the contribution of incident primary electrons to S.E.E., Rosler and Brauer (1981b) find that the proportion of the three yield contributions (plasmon decay, free electrons and core electrons) corresponds approximately to that of the reciprocal mean free paths for 1 to 2 keV (respectively 70% - 20% - 10% for Al at 2 keV).

Furthermore your model gives satisfactory value for the coefficient η of backscattered electrons ; but the compara tive yield for the production of a true SE between backscattered and primary electrons (β) is low compared to the experimental values.

Neverthless your calculated values for d are greater than the experimental ones and for Au and Cu, greater than the theoretical values at 1 keV obtained by Ganachaud (these) using a direct Monte Carlo simulation.

Could you comment on these remarks? What is the reason why the full width at half maximum is too low for the energy distribution of SE for AI (Fig.6)?

K.Murata: Could you comment on the reason of large discrepancies of the energy distribution of SEs for Al in Fig.6 from other results?

Authors: We agree with the point that the cascade process is over estimated, especially for low primary energy. In this paper the calculation of the high energy SE contribution in cascade process is performed rather approximately. The formula used for predicting the probability of SE formation during the cascade process, i.e., $\Delta E''/E$, which is based on spherically symmetric electron-electron collision in the center of mass system, is valid below 100 eV for SE, but it is used up to 2 keV. In fact above 100 eV it is more accurately described by Rutherford scattering rather than by Spherically symmetric scattering. This is the reason why the cascade process is over estimated, for example, our calculated values of δ for Au and Cu are greater than the experimental ones at 1 keV.

To improve this a more accurate model for calculation of SE including SE with energy (<100 eV) and (E_0>E>100 ev) has been performed. For SE with high energy we adopt the correct, Rutherford scattering, model to estimate the probability of producing new SE in a cascade process so the overestimation for SE in the cascade process has been reduced. Furthermore the maximum depth from which the SE are emitted is usually quoted as being about 50 Å below the surface in the case of metals (Koshikawa and Shimizu 1974, Chung and Everhart 1977), but this value does not take into consideration the contribution of internal secondaries generated with high energy deep in the sample. For a more accurate computation we have estimated the contribution of the region deeper than this maximum depth for SE emission. We think the contribution of SE with high energy (E_0>E>100eV) together with the contribution of SE deep in the sample have improved our model. Based on this new model the new calculated data for yield of SE, β coefficient and the energy distribution of SE are more favorable. So we believe that the shortage we have overcome in the new model is the reason why the yield of SE, the β coefficient and the energy distribution of SE for Al in Fig.6 have discrepancies.

In this work the contribution of fast secondary electrons generated from the interaction of primary electrons with core electrons is described by Gryzinski formula, which is used most frequently and is considered to be the most successful (Powell,1976) . Recently Ding and Shimizu (1988) assumed that the Gryzinski formula was also valid for " valence excitation" in their Monte Carlo study of backscattering and secondary electron generation and were successful . In our Fig.9 the percentage of SE from valence and core electrons for Al is not included the contribution of plasmon decay, if it is included, then the final percentage of SE from valence electrons,core electrons and plasmon decay is comparable to the data of

Rosler and Brauer (1981b). According to our calculation the proportion of the three yield contributions (plasmon decay, free electrons and core electrons) is 80%, 13.3% and 5.8%, respectively, for Al at 2keV. So we think that our calculated data for Al about the contribution of SE excited from core electron , which is carried out on Gryzinski formula, is reasonable . For Cu,Au and Ag because there is no suitable plasmon theory, the percentage of SE is not considered to include the contribution of plasmon decay. If the plasmon decay is included, we expect the data of contribution of core, d and valence electrons to be more favorable.

K.Murata: In Eqs.(1) and (2) you separated the energy range applicable into two regions using the value of 1.03J. But this causes an abrupt change in energy loss rate at this transition energy. In order to keep a smooth connection between both equations, the value of 6236 in Eq.(2) has to be changed although there may not be a large effect on the final results for high energy electrons. Could you comment on this? (note: If the value of 1.03J (actually 1.36J, I think) comes from Curgenven and Duncumb 1971, which gives the maximum in dE/ds, this must be 2.33J for 1.166 in the logarithmic term although the value can be arbitrarily taken).

Authors: The value 1.03J adopted in our model for 10,15,20 and 28 keV follows the value used by Chen and Mao(1983). They calculated the incident electron range by using

$$\text{Range} = \int_{1.03J}^{E_0} \frac{1}{dE/dS}\, dE \qquad (20)$$

where dE/dS is the Bethe formula. Physically the lower limit of integration should be zero, but for mathematical reasons E must be larger than J, so they took it 1.03J and using this model they got good results for the depth distributions of characteristic X-ray $\varphi(\rho z)$. For our SE calculation we use Eq.(2) to calculate the electron range from 1.03J down to zero. We agree that using this value causes an abrupt change in the energy loss rate at the transition energy. For example for Au at 1.03J by Eq.(1) the dE/dS is 1.36 eV/Å , by Eq.2 the dE/dS is 5.97 eV/Å(the difference is large, but not too large). According to Kotera et al. (1981, Fig.5), only from 1 keV there is apparently a difference of dE/dS between Eq.(1) and Eq.(2). It means that the discrepancy is only from 1.03J(0.82 keV) to 1 keV, which is not comparable to the whole energy range (from 0 to 10, 15, 20 and 28 keV). And using this model a good yield of backscattered electron can be obtained for all metal we calculated here. We agree with that even though to try to have a smooth connection between both equations, there may not be a large effect on final results for high energy electrons.

K.Murata: You mentioned you made the appropriate choice of the transition energy between the Bethe and Rao energy loss equations to obtain good agreement with the results with the Mott cross section. How was the transition energy chosen?

Authors: For 28, 20, 15 and 10 keV of incident electron energy, we use 1.03J as the transition energy, the reason is as above. Below 10 keV, the 6.34J is chosen as the transition energy. For example for Au from Kotera et al.(1981) Fig.5 it can be seen that the stopping power among Bethe formula,Rao-Sahib and Wittry and their model at 6.34J there is smooth and only a little difference at the energy range from 1 to 10 keV for all of them except Bethe formula.

L.Reimer: What is the total reflection of SE striking the surface with angles larger than the critical angle of total reflection.

Authors: In the elastic scattering process for the secondary electrons, the mean free path of the slow secondaries becomes as small as the order of atomic distance, this leads to an isotropic diffusion. Thus, all directions of motion of an internal SE at the surface are equally probable. In order for the SE with energy E at the surface to escape, we must have $E>E_F+\phi$. The maximum allowable value of θ for escape is determined by taking the normal component of momentum, $p\cos\theta$, equal to a value

$$p_c = \sqrt{2m(E_F+\phi)} \qquad (21)$$

Then the critical angle θc can be calculated from

$$\cos\theta_c = \frac{p_c}{p} = \frac{\sqrt{2m(E_F+\phi)}}{\sqrt{2mE}} = \sqrt{\frac{E_F+\phi}{E}} \qquad (22)$$

so

$$\theta_c = \cos^{-1}\sqrt{\frac{E_F+\phi}{E}} \qquad (23)$$

When an internal SE with energy E at the surface with $\theta > \theta c$, it will be back down into the sample to take part in cascade process. So for a SE with energy E at the surface there is a probability of

$$1-\sqrt{\frac{E_F+\phi}{E}} \qquad (24)$$

to escape to be a true SE; a probability of $\sqrt{(E_F+\phi)/E}$ to go back to take part in the cascade process in the sample.